

Effect of Impact Boeing 707-320 on External RC Containment of Nuclear Power Plant for Different Compressive Strength of Concrete

Mostafa Hassaan^{1*}, Mohamed Ihab ELMasry², Nabil Hassan EL Ashkar³

¹Research Assistant @ Ryerson University, Toronto –Ontario, Canada

²Professor of Structure Engineering @ AASTMT, Alexandria, Egypt

³Professor of Structure Engineering @ AASTMT, Alexandria, Egypt

DOI: [10.36348/sjce.2021.v05i08.004](https://doi.org/10.36348/sjce.2021.v05i08.004)

| Received: 18.08.2021 | Accepted: 24.09.2021 | Published: 27.09.2021

*Corresponding author: Mostafa Hassaan

Abstract

External RC containment vessel of nuclear power plant is considered as a vital structure in the nuclear plant. The main function for the external RC containment is to prevent the escape of radiation into the external environment. The external RC containment of NPPs is subjected to impact of an aeroplane Boeing 707-320 acting on 16 exterior nodes at a vertical distance of 30m measured from the top of the foundation level. The problem in this research is the damage generated due to the impact of missile on external RC containment which can escape the radiation into the external environment. The response for RC containment was conducted with respect to stresses, displacement, velocity and acceleration after the impact. The objective is to increase the compressive strength of concrete in order to reduce the damage for RC containment due to impact of missile compared to concrete with a compressive strength of 30 Mpa. It was observed that the damage affects only the impact region of the RC containment. Parametric numerical modelling was conducted using ANSYS program for concrete having different compressive strength for external RC containment. It was observed that the effect of different compressive strength has a great result on the displacement, velocity and acceleration for RC containment due to impact of Boeing 707-320.

Keywords: RC Containment, Impact of Boeing 707-320, Compressive Strength of Concrete.

Copyright © 2020 The Author(s): This is an open-access article distributed under the terms of the Creative Commons Attribution **4.0 International License (CC BY-NC 4.0)** which permits unrestricted use, distribution, and reproduction in any medium for non-commercial use provided the original author and source are credited.

1. INTRODUCTION

Nuclear Power Plants (NPPs) consist of multiple structures such as the internal and external containment structures. The external containment structure is the physical building (Primary) that separates the reactor from the outer atmosphere. Moreover, most typical current dimensions for external containment structures range between 150 to 200 feet tall with a diameter of approximately 150 feet according to ASCE 58 (1980), (CZERNIEWSKI, 2009). The external RC structure should be designed in order to prevent the release of radioactive particles into the atmosphere. The secondary containment is important when radiation levels at the site boundary exceed the allowable limits (CZERNIEWSKI, 2009). In addition, most current external containment structures are designed as RC structures. Nuclear power plants are recognised to have a robust structure, therefore the impact of a fully loaded aeroplane would not be expected to damage the containment of a reactor building which at present would be a double containment made of heavily steel bar reinforced

concrete with thickness of more than one metre (Forasassi and Lofrano, 2010). The impact load due to the effects of a finite amount of kinetic energy depends on the inertial and stiffness properties of missile and target structure (Forasassi and Lofrano, 2010). As a result of the impact of an aeroplane, kinetic energy is transferred from the aeroplane to the building walls and absorbed by the building components in the form of strain energy while each component is deforming elastically and beyond up to the point of permanent yielding.

The behaviour of these structures could be considered as elastic with no occurrence of permanent damage to the structures. The reinforced concrete containments with thicknesses greater than 1.4 m permanent damage is negligible due to impact of an aeroplane while for thicknesses lower than one-meter considerable plastic strains occurred (Němec *et al.*, 2012) on the opposite surfaces of the containment shell different signs of strain are obtained with negative sign prevailing (Němec *et al.*, 2012). The problem is

considered in this research as nonlinear transient dynamics problems. As the method was seen to have all the advantages of the explicit scheme as long as the damping matrix $C=0$ or $C=\alpha M$, Raileigh damping with coefficient $\beta=0$ was applied to the model. The coefficient α was reflected with a magnitude of 3.0 for the reinforced concrete and 0.1 for the structural steel as in equation (1). In the impact analysis, the damping effect was considered to be negligible as it does not affect the maximum response to impulse loading (Němec *et al.*, 2012).

$$C=\alpha M+\beta K \dots\dots\dots \text{Eq. (1)}$$

Moreover, concrete is commonly used as a construction material for biological shielding in nuclear power plants. Biological shields must consider in the design x-rays and gamma ray's emissions. Mehta and Monteiro (2006) stated that concrete is an excellent shielding material that possesses the needed characteristics for both neutron and gamma ray attenuation which has satisfactory mechanical properties and has a relatively low initial as well as maintenance costs.

1.1 Research Objective

This research studies the response caused by an aeroplane impact, namely Boeing 707-320, for a typical outer RC containment of the new generation of NPPs. The step-by-step nonlinear response of such impact is studied then analysed to identify the extent of damage due to the effect of impact of an aeroplane. Moreover, different models were made with different compressive strength of concrete which is affected by impact of an aeroplane Boeing 707-320 in order to deduct the impact influence on the external RC containment on displacement, velocity, acceleration and shape of the cracks. Compressive strength of concrete affects the quantity of damage for external RC containment. Increasing the compressive strength can reduce the effect of damage and the possibility of leakage of radiation into the external environment. Moreover, considering on this study the effect of inner steel liner plate on displacement, velocity and acceleration of containment and comparing it to model which doesn't contain inner steel liner plate having a compressive strength of 60 Mpa.

1.2 RESEARCH METHODOLOGY

Numerical models were conducted using ANSYS software and the load of an aeroplane was deducted using Riera method. The external RC containment was simulated for different concrete compressive strength. The connection of RC wall of the containment with the foundation is assumed to be fixed in the model.

2 Modelling of the External RC Containment

2.1 Finite Element Modelling of RC Containment

Typical RC nuclear containment consists of a wall, dome and base mat foundation. Thickness of the

wall was taken 1.2m according to ASCE 58 (1980). The dome was carried by the wall and the load of the wall was transmitted into the foundation (CZERNIEWSKI, 2009). The inner diameter of the containment was considered 45m and the height of cylindrical wall is 36.45m from the top of foundation level. The total height of the containment was considered 60m height as shown in Fig.1. In the recent model considering the connection between the foundation and cylindrical wall is fixed connection. The reinforcement was considered in this model concentrated at membrane layers inside the wall and dome, specifying for these layers by the material number and the direction of reinforcement by 2 angles (theta, phi). The reinforcement layers were considered continuous along the length of each layer (Forasassi and Lofrano, 2010). Reinforcement of the wall is #40mm at 80mm in the direction of vertical, while in the direction of circumference the reinforcement is considered #40 mm at 80mm according to Abbas *et al.*, (1996), Saberi *et al.*, (2017). The mesh of the element in this model is conducted for the wall and the dome using ANSYS as shown in Fig 2.

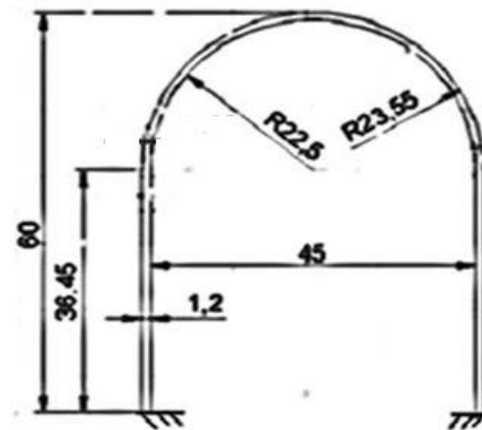


Fig 1: Geometrical of Typical External RC Containment

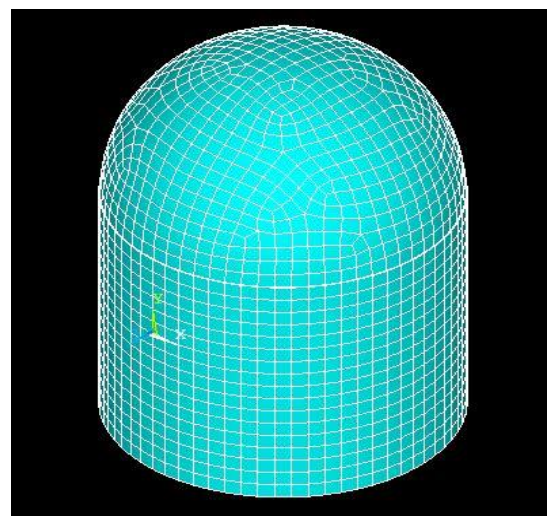


Fig 2: Meshing for External RC Containment using ANSYS

2.2 Material Modelling of the RC External Containment

Concrete and steel reinforcement have different material modelling. Concrete material has been modelled as a multi linear isotropic hardening plasticity having its stress strain curve as shown in Fig 3 (Salman, 2015). Non-linear curve of concrete was calculated from equation (2) to equation (6).

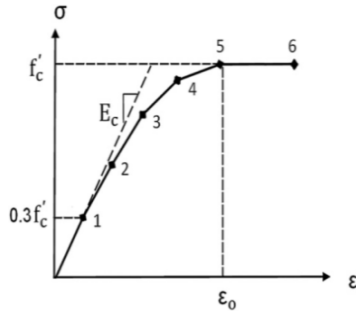


Fig 3: Uniaxial Compressive Stress Strain Curve for Concrete in Compression

$$f_c = E_c \varepsilon \text{ for } 0 < \varepsilon < \varepsilon_1 \dots \dots \dots \text{Eq. (2)}$$

$$f_c = f'_c \text{ for } \varepsilon_0 < \varepsilon < \varepsilon_{cu} \dots \dots \dots \text{Eq. (3)}$$

$$f_c = \frac{E_c \varepsilon}{\left(1 + \left(\frac{\varepsilon}{\varepsilon_0}\right)^2\right)} \text{ for } \varepsilon_1 < \varepsilon < \varepsilon_0 \dots \dots \dots \text{Eq. (4)}$$

$$\varepsilon_1 = (0.3 \times f'_c) / (E_c) \dots \dots \dots \text{Eq. (5)}$$

$$\varepsilon_0 = (2f'_c) / (E_c) \dots \dots \dots \text{Eq. (6)}$$

Poisson ratio for concrete is taken 0.17 and its elastic modulus can be calculated from the following equation (7) according to ACI 318 (2008) and (Salman, 2015).

$$E_c = 4700 \sqrt{f'_c} \dots \dots \dots \text{Eq. (7)}$$

The concrete also has a non-metal plasticity as shown in Table 1. The uniaxial cracking tensile stress for concrete can be calculated from the following equation (8) according to ACI 318 (2008) and Saberi *et al.*, (2017). The material modelling of concrete in tension was modelled as shown in Fig 4.

$$f_r = 0.62 \sqrt{f'_c} \dots \dots \dots \text{Eq. (8)}$$

Table 1: Concrete Input Data

Input strength parameters	Values
Open shear transferee coefficient	0.3
Closed shear transferee coefficient	0.9
Poisson ratio of concrete	0.17

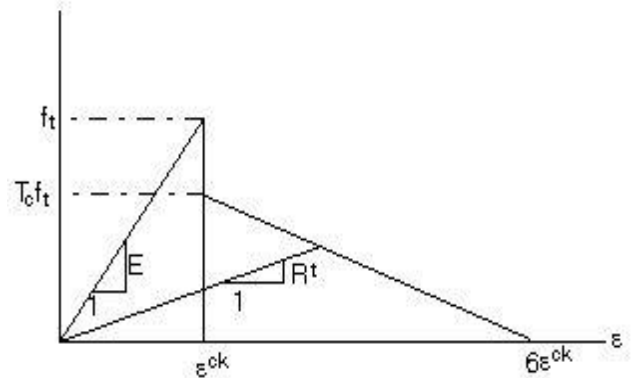


Fig 4: Stress Strain Curve for Concrete in Tension (ANSYS 12.1)

The material modelling of steel reinforcement is elastic perfectly plastic as shown in Fig 5. The elastic modulus is taken $2E5 \text{ N/mm}^2$ and its Poisson ratio is 0.33, while the steel reinforcement is treated as bilinear isotropic hardening plasticity its yielding is 490 Mpa (Saberi *et al.*, 2017). The density of steel reinforcement and steel liner plate was taken 7850 Kg/m^3 .

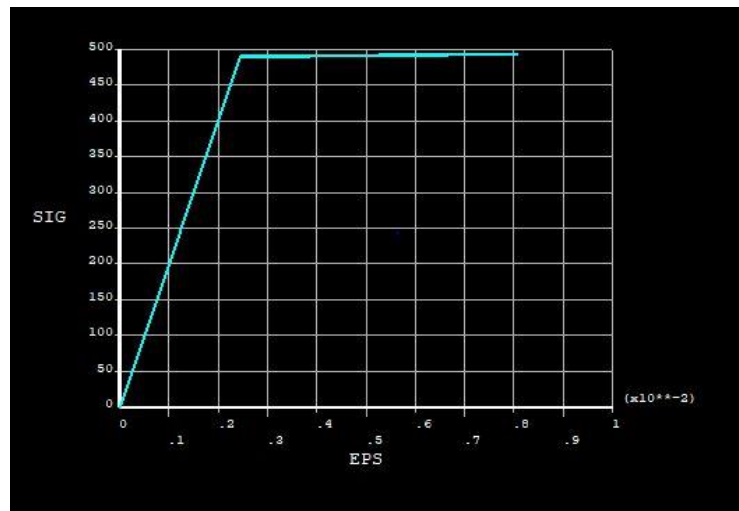


Fig 5: Stress Strain Curve for Steel Reinforcement

The elastic modulus and rupture strength of concrete were calculated for different compressive strength (30Mpa, 45Mpa, 60Mpa and 75Mpa) as shown

in Table 2, which is a parametric study for RC containment models which is subjected to impact of an aeroplane Boeing 707-320.

Table 2: Concrete Material Properties for Different Compressive Strength

Fc (Mpa)	Ec (N/mm ²)	fr (N/mm ²)	Density (kg/m ³)
30	25743	3.286	2400
45	31528.558	4.159	2400
60	36406.043	4.8	3000
75	40703.19	5.369	3000

2.3. Elements Model Used from ANSYS® Library

2.3.1. SOLID65 element

SOLID65 element is used for the 3D modelling of the RC wall and dome. The solid element is capable of cracking in tension and crushing in compression. The element is defined by eight nodes having three degrees of freedom at each node:

translations in the nodal X, Y and Z directions and the isotropic material properties. The element has one solid material and up to three rebar materials as shown in Fig. 6. The orientation of any rebar layer is defined by two angles in degrees from the element coordinate system (ANSYS 12.1).

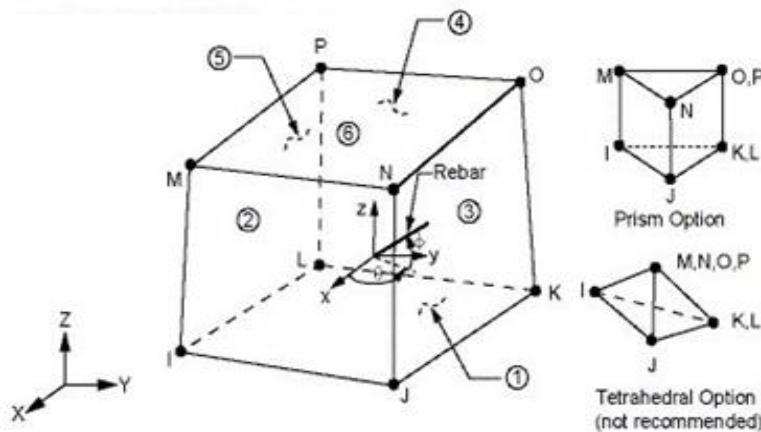


Fig 6: Solid 65 Element (ANSYS 12.1)

In addition, SOLID65 allows the presence of four different materials within each element; one matrix material as concrete, and a maximum of three independent reinforcing materials. The concrete material is capable of directional integration point cracking and crushing besides incorporating plastic and creep behaviour. The reinforcement which also incorporates creep and plasticity has uniaxial stiffness only and is assumed to be smeared throughout the element.

The other assumptions include that the concrete material is homogenous and isotropic where cracking is permitted in three orthogonal directions at each integration point. In addition, if cracking occurs at an integration point, the cracking is modelled through

an adjustment of material properties that effectively treats the cracking as a smeared band of cracks, rather than discrete cracks. Moreover, the reinforcement is assumed to be “smeared” throughout the element.

2.4 Failure criteria

The concrete material model predicts the failure of brittle materials. Both cracking and crushing failure modes are accounted for.

The criterion for failure of concrete due to a multi-axial stress state can be expressed in the following equation (9) (William and Warnke, 1974):

$$\frac{F}{f_c} - s \geq 0 \dots\dots\dots \text{Eq.(9)}$$

Where:

F = a function of the principal stress state (σ_{xp} , σ_{yp} , σ_{zp})
S = failure surface expressed in terms of principal stresses and five input parameters f_t , f_c , f_{cb} , f_1 and f_2
f_c = uniaxial crushing strength
σ_{xp} , σ_{yp} , σ_{zp} = principal stresses in principal directions

If equation (9) is satisfied, the material will crack or crush. However, the failure surface can be specified with a minimum of two constants, f_t and f_c .

However, the failure surface can be specified with a minimum of two constants, f_t and f_c as shown in equation (11) to equation (13) (William and Warnke, 1974).

$$f_{cb} = 1.2 f_c \dots\dots\dots \text{Eq. (11)}$$

$$f_t = 1.45 f_c \dots\dots\dots \text{Eq. (12)}$$

$$f_2 = 1.725 f_c \dots\dots\dots \text{Eq. (13)}$$

These default values are valid only for stress states where the condition is satisfied as shown in equation (14) and equation (15).

$$|\sigma_h| \leq \sqrt{3} f_c \dots\dots\dots \text{Eq. (14)}$$

$$\sigma_h = \text{hydrostatic stress state} = 1/2(\sigma_{xp} + \sigma_{yp} + \sigma_{zp}) \dots\dots\dots \text{Eq. (15)}$$

Both the function F and the failure surface S are expressed in terms of principal stresses denoted as σ_1 , σ_2 , and σ_3 where: $\sigma_1 = \max(\sigma_{xp}, \sigma_{yp}, \sigma_{zp})$, $\sigma_3 = \min(\sigma_{xp}, \sigma_{yp}, \sigma_{zp})$ and $\sigma_1 \geq \sigma_2 \geq \sigma_3$. The failure of concrete is categorized into four domains:

1. $0 \geq \sigma_1 \geq \sigma_2 \geq \sigma_3$ (compression - compression - compression)
2. $\sigma_1 \geq 0 \geq \sigma_2 \geq \sigma_3$ (tensile - compression - compression)
3. $\sigma_1 \geq \sigma_2 \geq 0 \geq \sigma_3$ (tensile - tensile - compression)
4. $\sigma_1 \geq \sigma_2 \geq \sigma_3 \geq 0$ (tensile - tensile - tensile)

2.5 Modelling the Impact of an Aeroplane Boeing (707 -320) and Airbus (A-320)

The Riera method (Riera, 1968) constructing a force time history to simulate an aeroplane crash impact has long been accepted for use in the accident analysis due to an aeroplane crash impact. This is an approximate method for constructing a force time history for a missile striking a rigid wall based on a known distribution of mass and crushing characteristics of the missile along the length (James and Rashid, 2005).

The basic assumptions of the Riera method are: the target is rigid; the axis of the missile is perpendicular to the target; the missile is separated into two regions, one being uncrushed and moving with velocity and the other region being crushed with zero velocity; all crushing takes place within a local region adjacent to the rigid target; the crushing or material behaviour of the missile is rigid perfectly plastic. The important parameters that affect the accident scenario for an aeroplane impact are Velocity and impact angles of the aeroplane; Mass and stiffness; Size and location of the impact area.

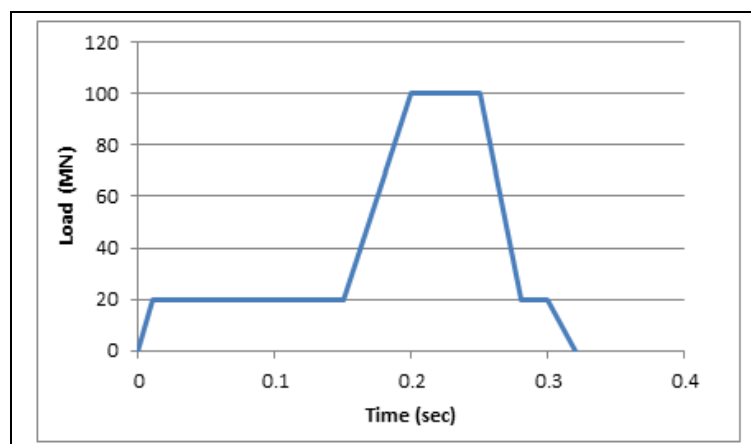
The mass of the impact missile within a lamina adjacent to the rigid target wall is crushed and brought to rest, resulting in a change of momentum. The resulting dynamic force is then applied to the wall along with the force required to crush the lamina of the missile. The crushing force component then acts to decelerate the remaining uncrushed missile mass.

The key formula in the computation of the force applied to the rigid target, $F(t)$, or the impact force time history is given by equation (16) (James and Rashid, 2005).

$$F(t) = P_c(x) + \mu(x) (dx/dt)^2 \dots\dots\dots \text{Eq. (16)}$$

Where $x(t)$ is the crushed length of the missile, (the distance from the nose of the missile when uncrushed to the point at which crushing has progressed at time t), $P_c(x)$ is the static force required to axially crush a cross-section of the missile at location x , and $\mu(x)$ is the mass per unit length at location x .

The load time curve for an aeroplane impact of Boeing 707-320 moving at a speed of 103 m/sec is applied in the numerical model acts at 16 nodes as concentrated load. The assumed contact area is 28 m² (Riera, 1968). The load is transient dynamic analysis at which the load of impact changes with respect to time as shown in Fig 7(a). The distributions of loads are distributed in each load step according to the distribution as shown in Fig 7(b).



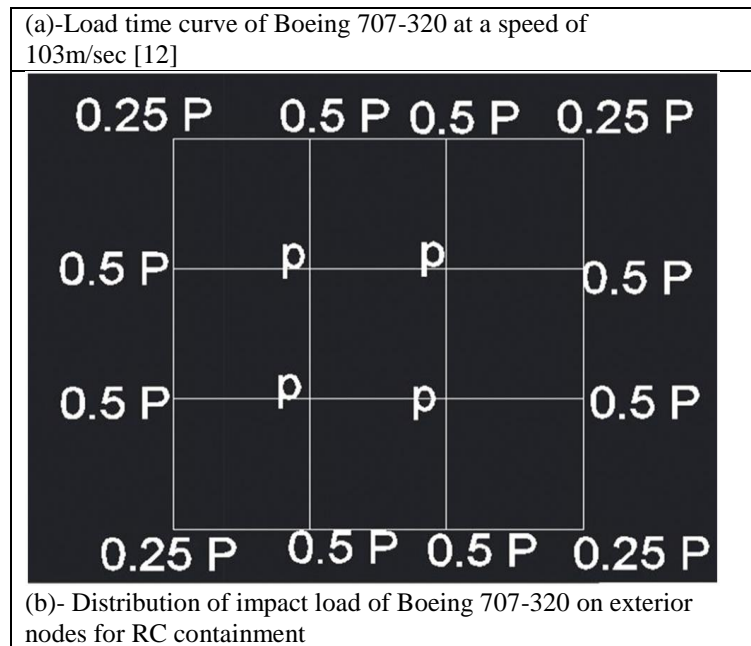


Fig 7: Load Time Curve for Boeing 707-320 and its Distribution on RC containment

In addition, the load time curve for impact of an aeroplane Air bus A-320 moving at a speed of 120 m/sec is applied in the numerical model act at 16 nodes as concentrated load as a verification model on this

research paper. The assumed contact area is 28 m² according to Siefert and Henkel (2013). The load is transient dynamic analysis at which the load of impact changes with respect to time as shown in Fig 8.

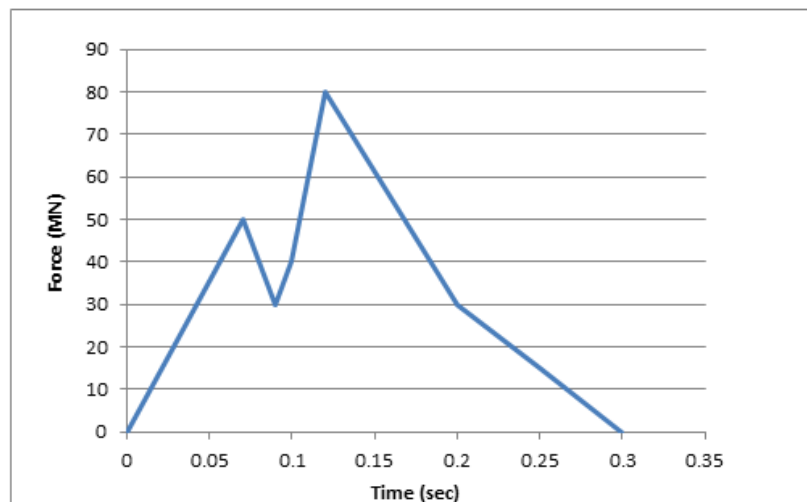


Fig 8: Load Time Curve for Air bus A-320 moving at a speed of 120 m/sec (Siefert and Henkel, 2013)

2.6 Verification of Model

For Boeing 707-320 aeroplane, the maximum displacement was found to be 34.2 mm by Abbas *et al.*, (1996), Verification of modelling, the model has been verified using impact of an aeroplane Boeing 707-320 moving with a speed of 103 m/sec hitting the outer nodes of the external RC containment with an impact region of 28 m². Moreover, the maximum displacement at the nodes of impact due to impact of Boeing 707-320 aeroplane was found to be 37.854mm towards the direction of loading as shown in Fig 9(a) which

corresponds to the maximum displacement of 35.37 mm which was conducted by Saberi *et al.*, (2017). Another model has been verified by using impact of Air bus A-320 moving with a speed of 120 m/sec on the outer nodes of the external containment with an impact region area of 28 m². It was found that the maximum displacement within the impact region for impact of air bus A-320 aeroplane is 28.68 mm as shown in Fig 9-(b) which corresponds to the maximum displacement conducted by Saberi *et al.*, (2017) which is 28.38 mm at a vertical height of 30m.

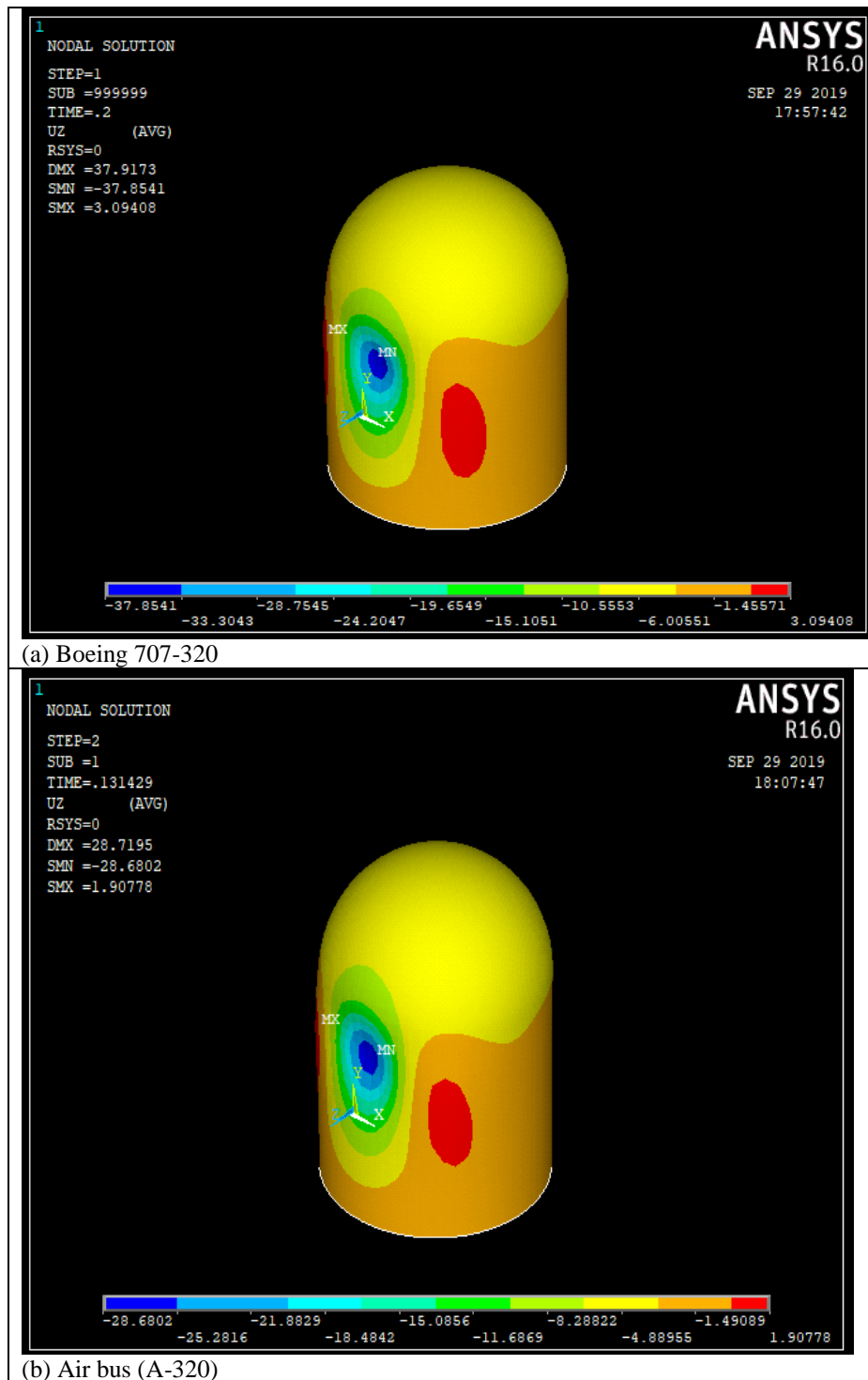


Fig 9: Displacement of RC Containment for Different Aeroplanes Impact

3. Analysis of Results

The outer RC containment response under impact of Boeing 707-320 aeroplane impact load was studied at different time instances. Fig 10(a) shows the deformation schematic of the exterior RC containment within the impact region at time of 0.2second. It can be concluded that the elements within the impact region deformed in the direction of loading, which generated

significant large tensile stresses at the inner surface of reinforced concrete. The maximum displacement due to the impact of Boeing 707-320 on the exterior RC containment was found to be 42.0305 mm in the region of impact at time of 0.2 second. Meanwhile, other regions near the impact showed maximum displacements of 6.5 mm outside the containment in a normal 90° incidence manner as shown in Fig 10(b).

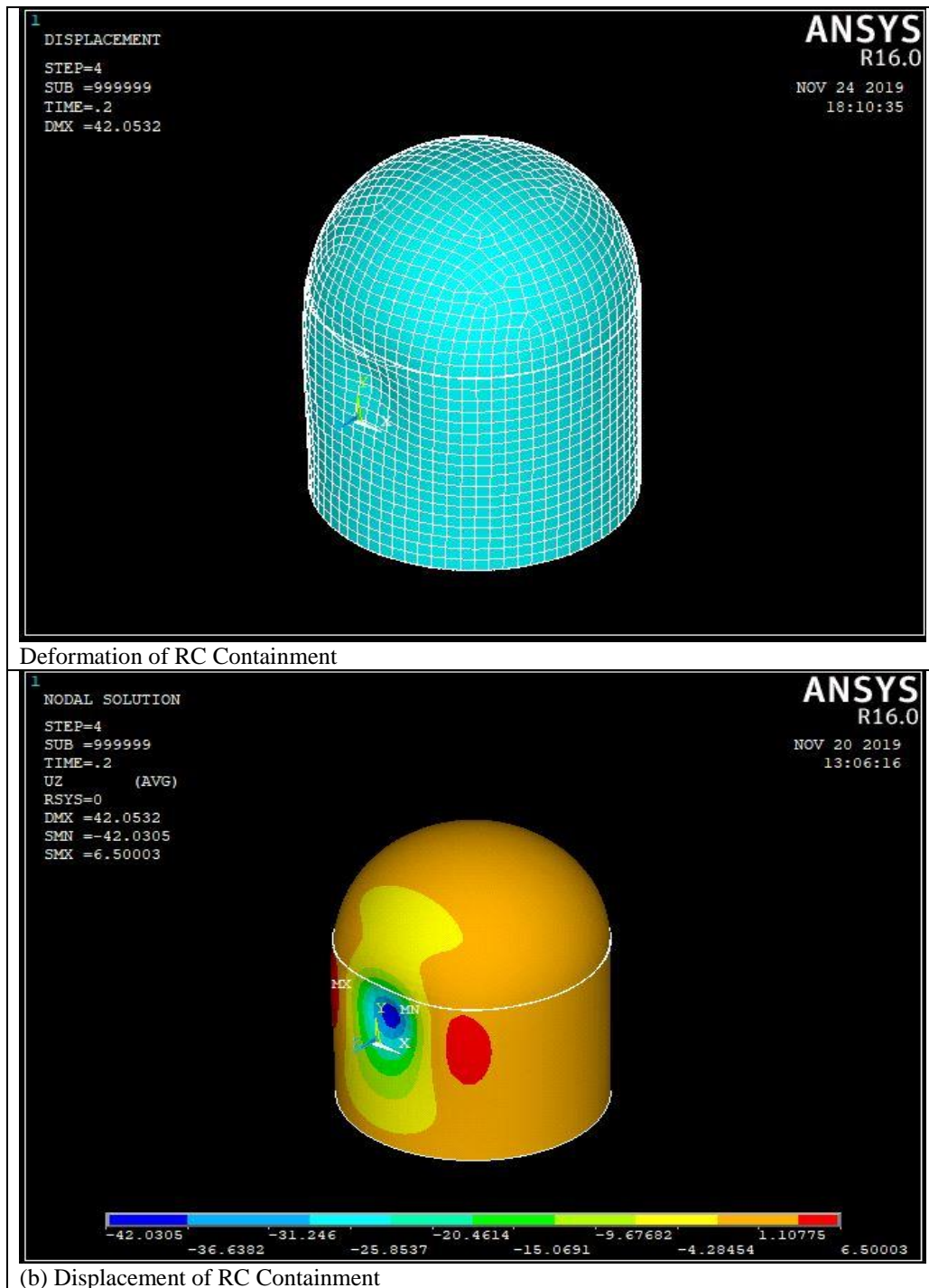


Fig 10: Deformation and Displacement of RC Containment due to Impact of an Aeroplane Boeing 707-320 at Time of 0.2 Second

The velocity of the RC containment is -1214.86 mm/sec within the impact region towards the direction of loading as shown in Fig 11(a) due to the impact of an aeroplane Boeing 707-320 at a vertical distance of 30 m measured from the top of foundation level. Moreover, the velocity reached a value of 240.298mm/sec outwards the plane of the RC

containment away from the impact region as shown in Fig 11(a). In addition, it was observed that from ANSYS, the analysis for the four exterior nodes which carry maximum load of impact carry a velocity of value -1214.86 mm/sec at time of 0.2 second as shown in Fig 11(b).

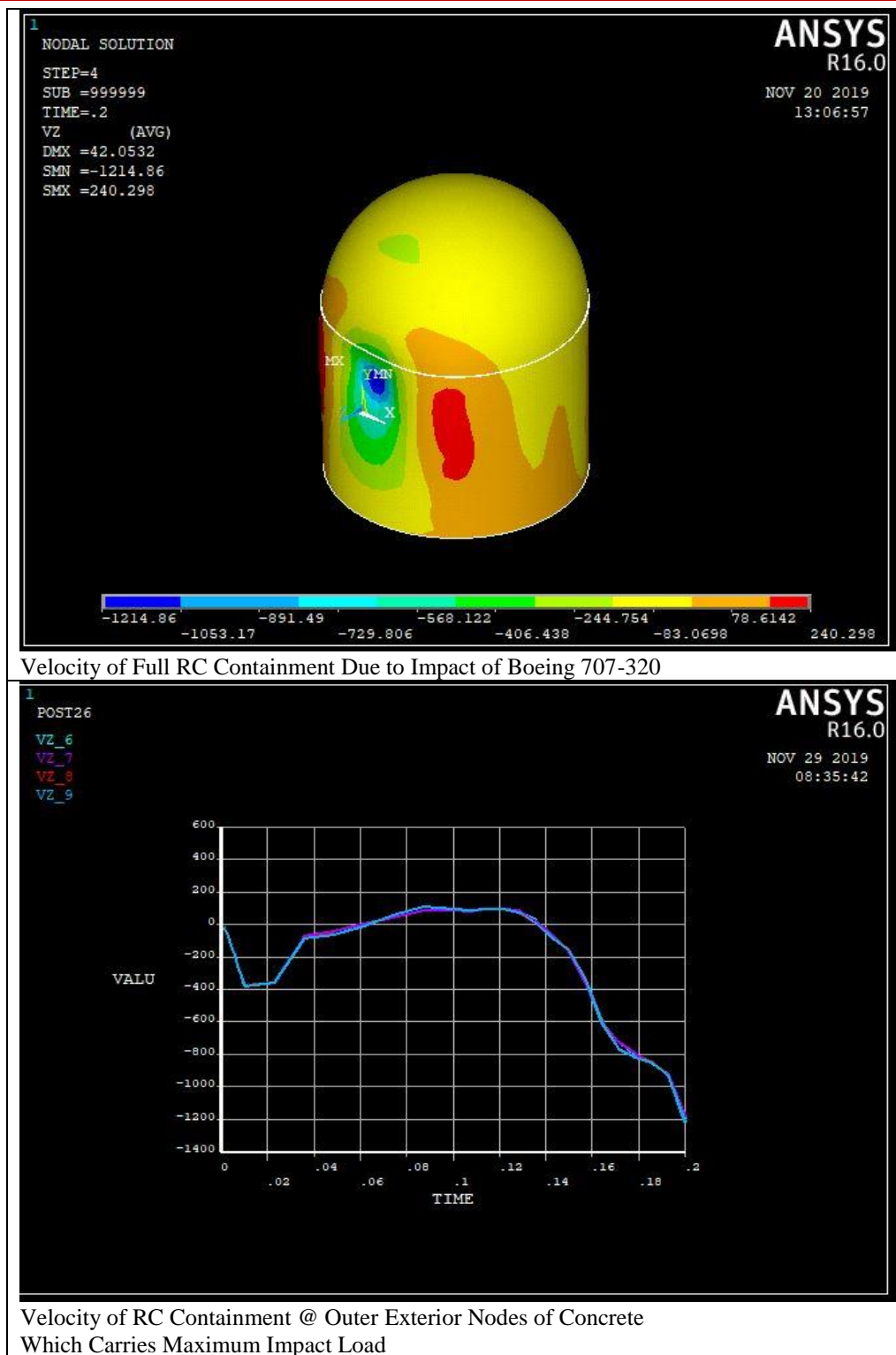


Fig 11: Velocity of RC Containment Due to Impact of an Aeroplane Boeing 707-320 at Time 0.2 second

The acceleration of the RC containment reached a value of -40000 mm/sec^2 towards the direction of loading within the impact region as shown in Fig 12(a) due to the impact of an aeroplane Boeing 707-320 at a vertical distance of 30 m. Moreover, it was

concluded that from ANSYS, the four exterior nodes at concrete which carry maximum load of impact carry an acceleration value of -40000 mm/sec^2 at time of 0.2 second as shown in Fig 12(b).

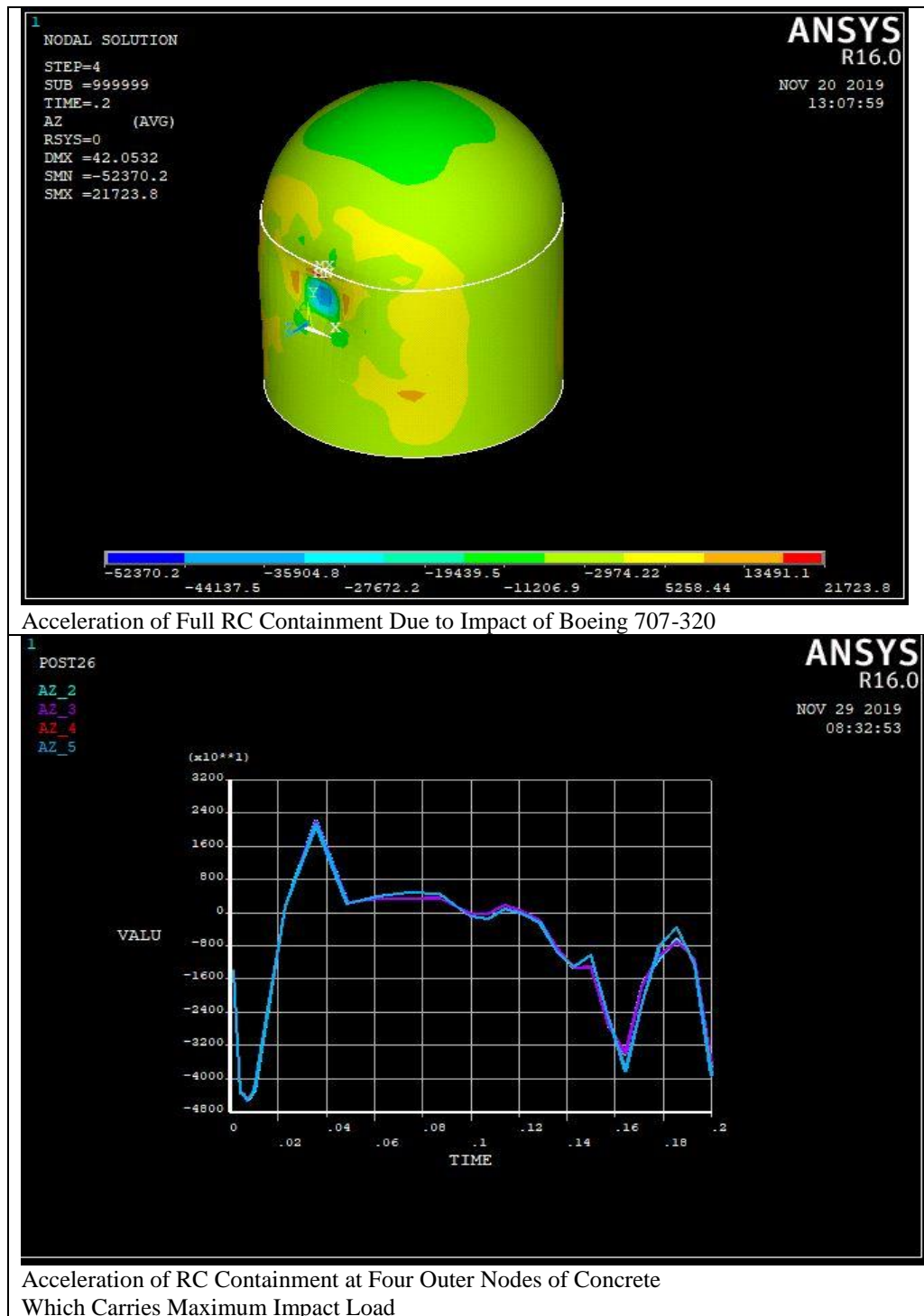
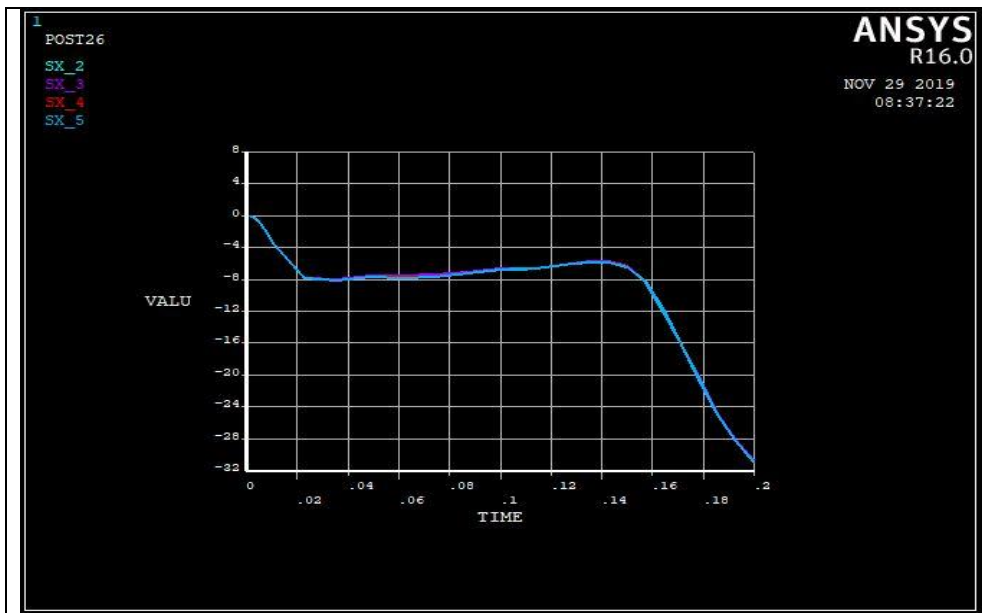


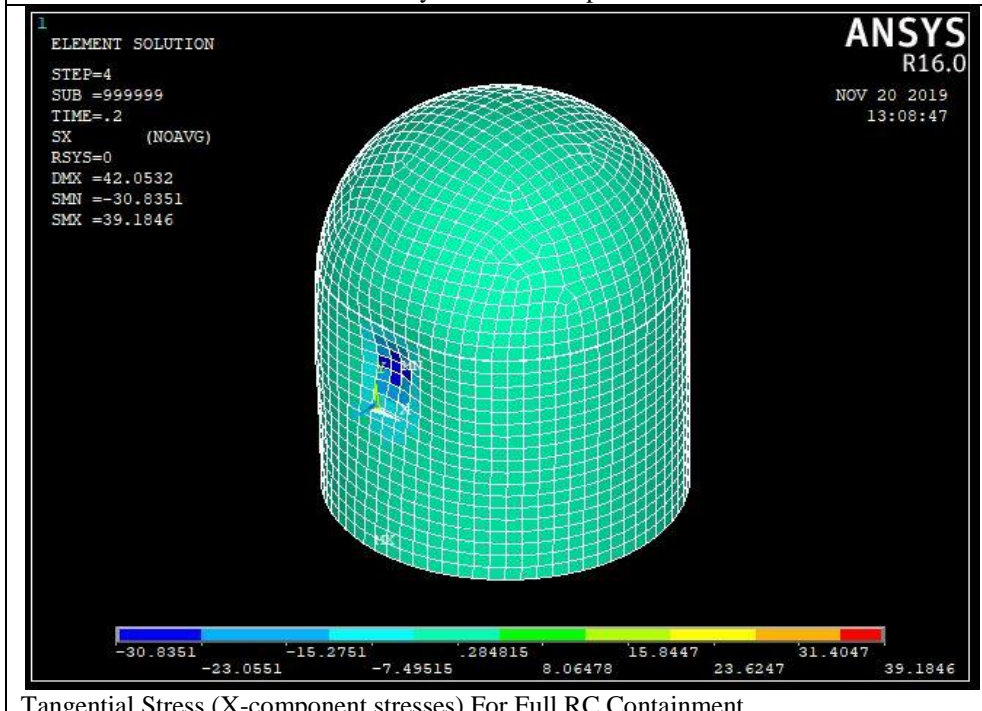
Fig 12: Acceleration of RC Containment Due to Impact of an Aeroplane Boeing 707-320 @ Time 0.2 Second

The four outer nodes which carry maximum impact load within the impact of an aeroplane its local tangential stress (x component stress) of concrete within the impact region reached a value of -30 Mpa as shown

in Fig 13(a). This means that concrete has been crushed at its outer nodes of the maximum impact load. Thus, the element which suffered the impact load of an aeroplane is fully damaged as shown in Fig 13(b).



Tangential Stress (X Component Stresses) of RC containment at The Outer Nodes of Concrete Which Carry Maximum Impact Load



Tangential Stress (X-component stresses) For Full RC Containment

Fig 13: Tangential Stress (X Component Stress) For the Containment @ Time of 0.2 Second of impact

It was observed that at the inner nodes of concrete within the impact region carries the maximum tensile stress according to the principle tensile stress as shown in Fig 14. According to the failure criteria of concrete which was applied on the inner concrete nodes

within the impact region, from 1st, 2nd and 3rd principle stresses, the concrete is cracked at the inner surface of impact region in direction perpendicular to the 1st and 2nd principle stresses according to the failure criteria of concrete.

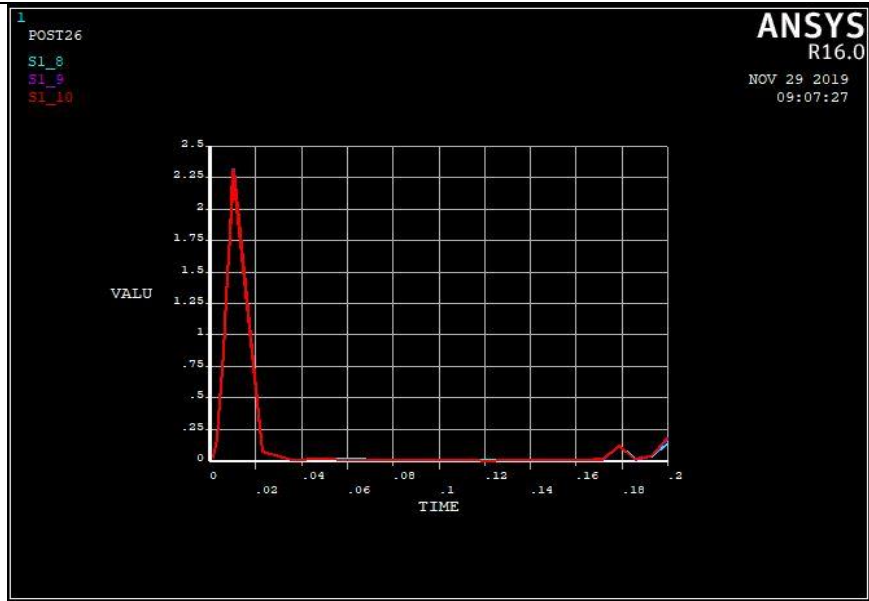
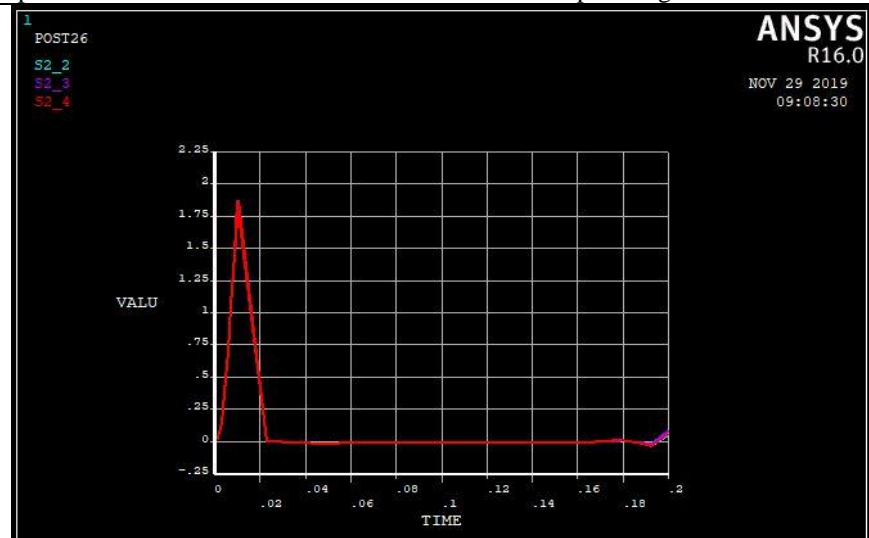
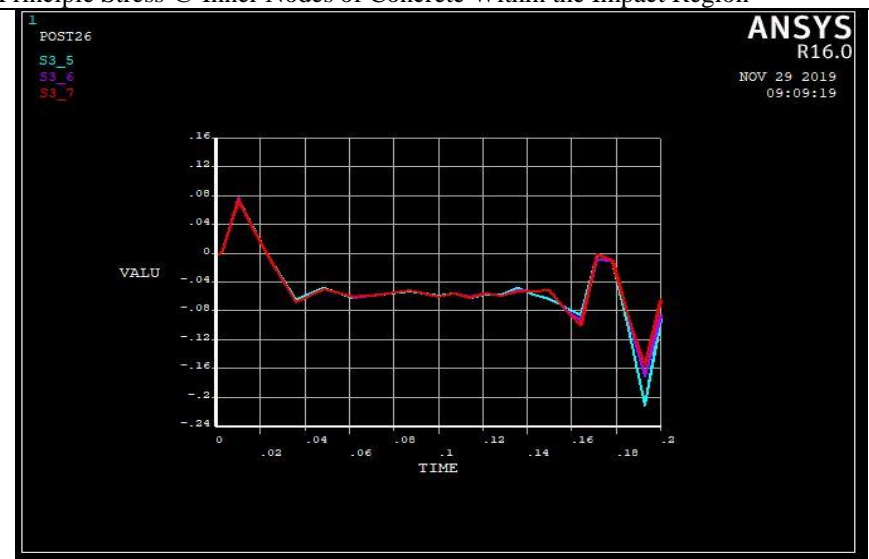

1st Principle Stress @ Inner Nodes of Concrete Within the Impact Region

(b) 2nd Principle Stress @ Inner Nodes of Concrete Within the Impact Region

(c) 3rd Principle Stress @ Inner Nodes of Concrete Within the Impact Region

Fig 14: Principle Stresses @ Four Inner Nodes of Concrete within the Impact Region @ time 0.2 second of Impact

The tangential strain (x component strain) reached a value of $1.7\text{E-}3$ at the inner nodes of concrete within the impact region. This means that the inner

nodes of concrete within the impact region were cracked as shown in Fig 15.

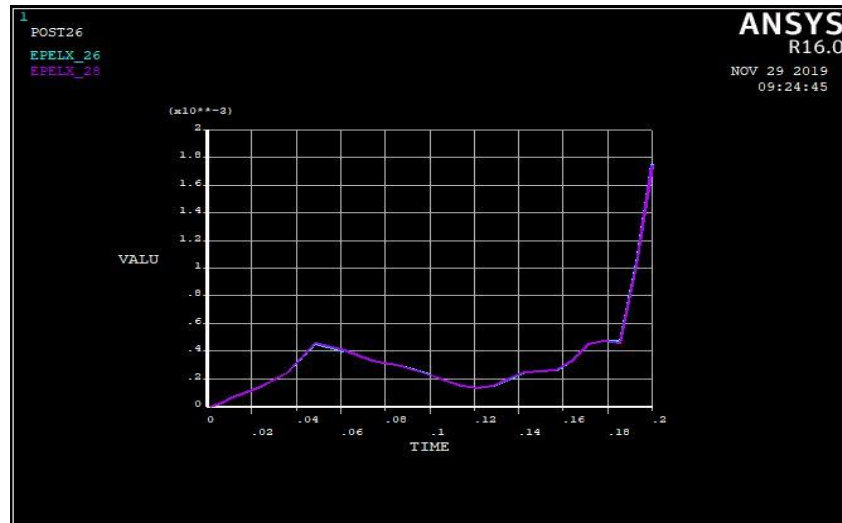


Fig 15: X-Component Elastic Strain @ the Inner Nodes of Concrete within the Impact Region @ time 0.2 second

Based on the previously mentioned results, thus, the elements within the impact region were clearly crushed. In addition, some tension cracks (flexure cracks) appeared at the bottom of the fixation of the RC

containment with the foundation. Moreover, shear cracks appeared far from the impact region as shown in Fig 16.

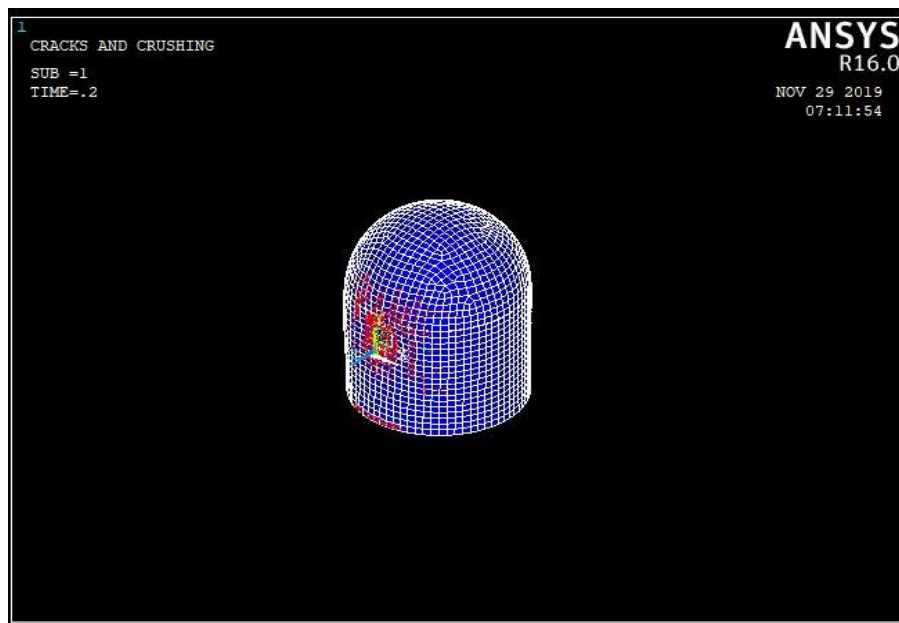


Fig 16: Crack Propagation Within the RC Containment due to Impact of an Aeroplane Boeing 707-320

The impact of an aeroplane Boeing 707-320 moving with a speed of 103 m/sec hitting the external RC containment of nuclear power plant at a vertical distance of 30 m measured from top of foundation level with different models of different compressive strengths includes (30-45-60 -75) Mpa. The maximum displacement of RC containment is 42.031mm in

direction of impact within the impact region for a concrete with compressive strength of 30 Mpa as shown in Fig 17(a) and Fig 18. The displacement of RC containment is 28.08 mm in direction of impact within the impact region for a concrete with compressive strength of 75 Mpa as shown in Fig 17(d) and Figure 18.

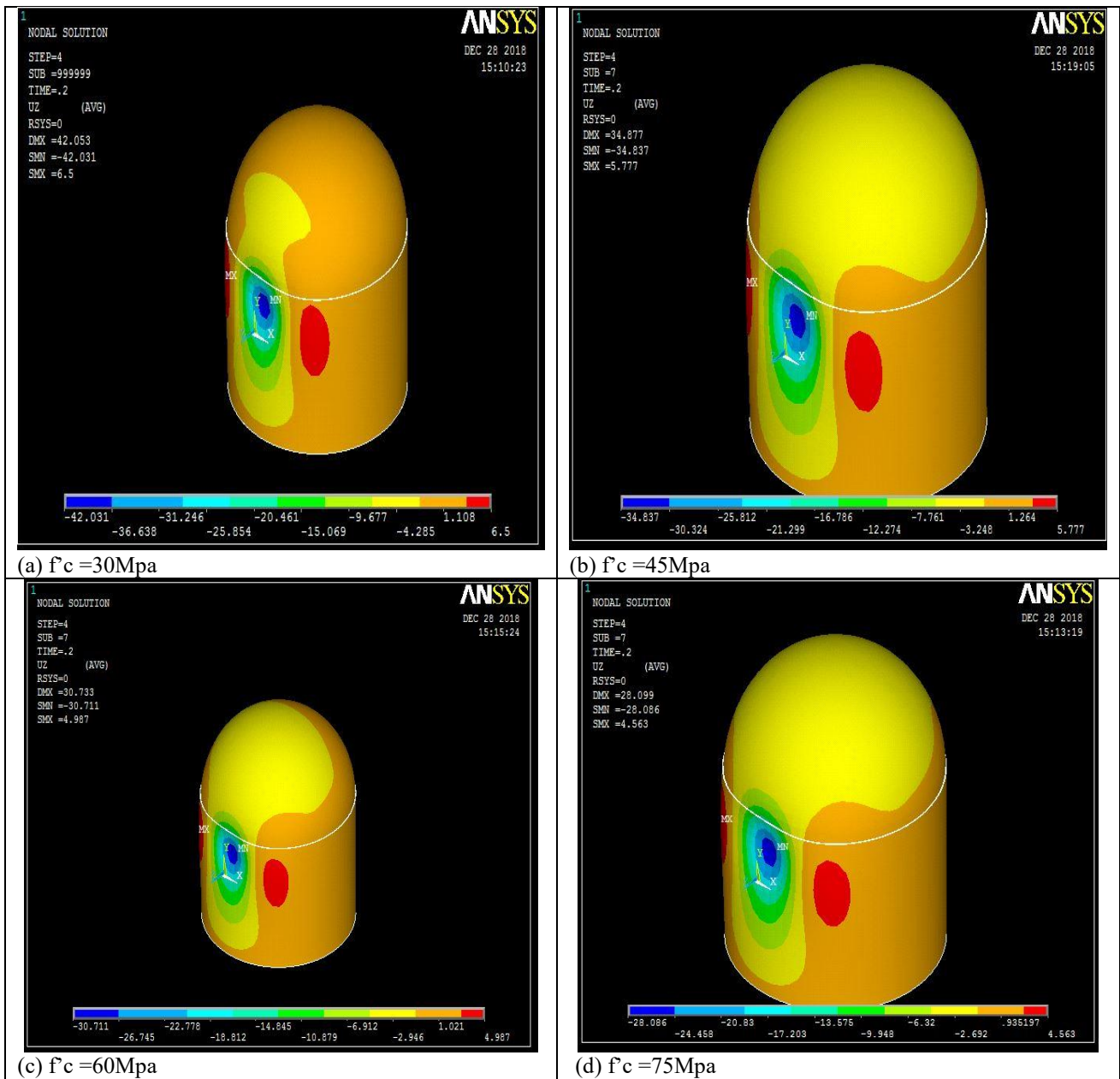


Fig 17: Displacement of RC Containments for Concrete with Different Compressive Strength

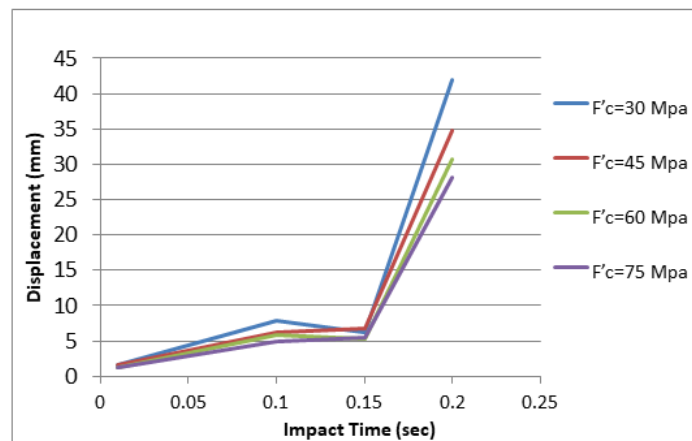


Fig 18: Displacement of RC Containments for Concrete with Different Compressive Strength with Respect to Time of an Aeroplane Impact (Boeing 707-320)

Displacement of RC containment is 42.03mm when the compressive strength is 30 Mpa. Moreover, displacement of RC containment is 28.086mm when the compressive strength is 75 Mpa. The percentage of decrease in displacement value from 30 Mpa to 75 Mpa

by 49.6% as shown in Fig 19. It is strongly recommended to make a compressive strength for the external RC containment vessels higher than 75 Mpa in order to reduce the displacement due to impact of an aeroplane Boeing 707-320.

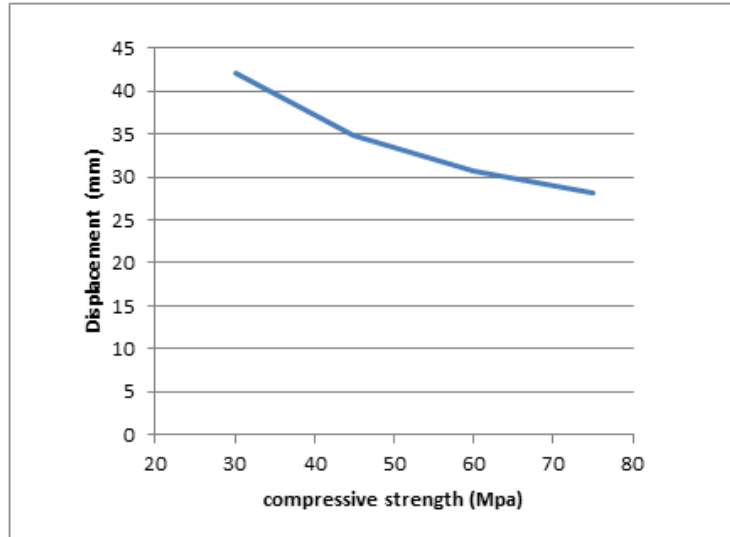


Fig 19: Displacement of RC Containment Versus Different Compressive Strength due to Impact of Boeing 707-320 @ time of impact 0.2 second

The maximum displacement of RC containment due to impact of Boeing 707-320 is within the impact region and the displacement vanishes after 20m away from the impact region from each side as

shown in Fig 20. The maximum displacement is 41.67 mm when the compressive strength is 30 Mpa, while when the compressive strength is 75 Mpa, the maximum displacement is 28 mm.

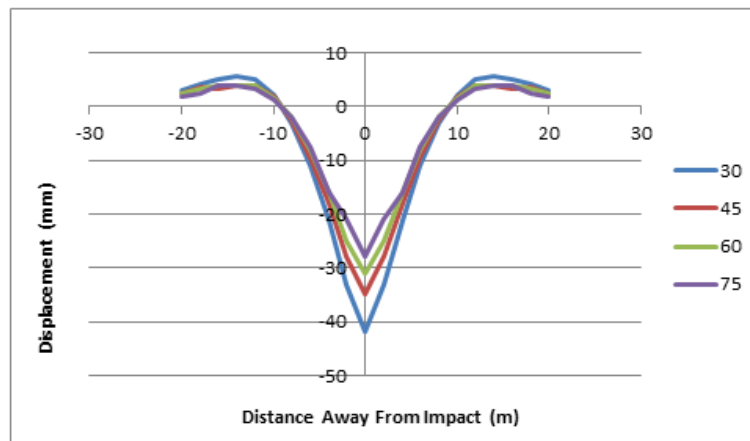
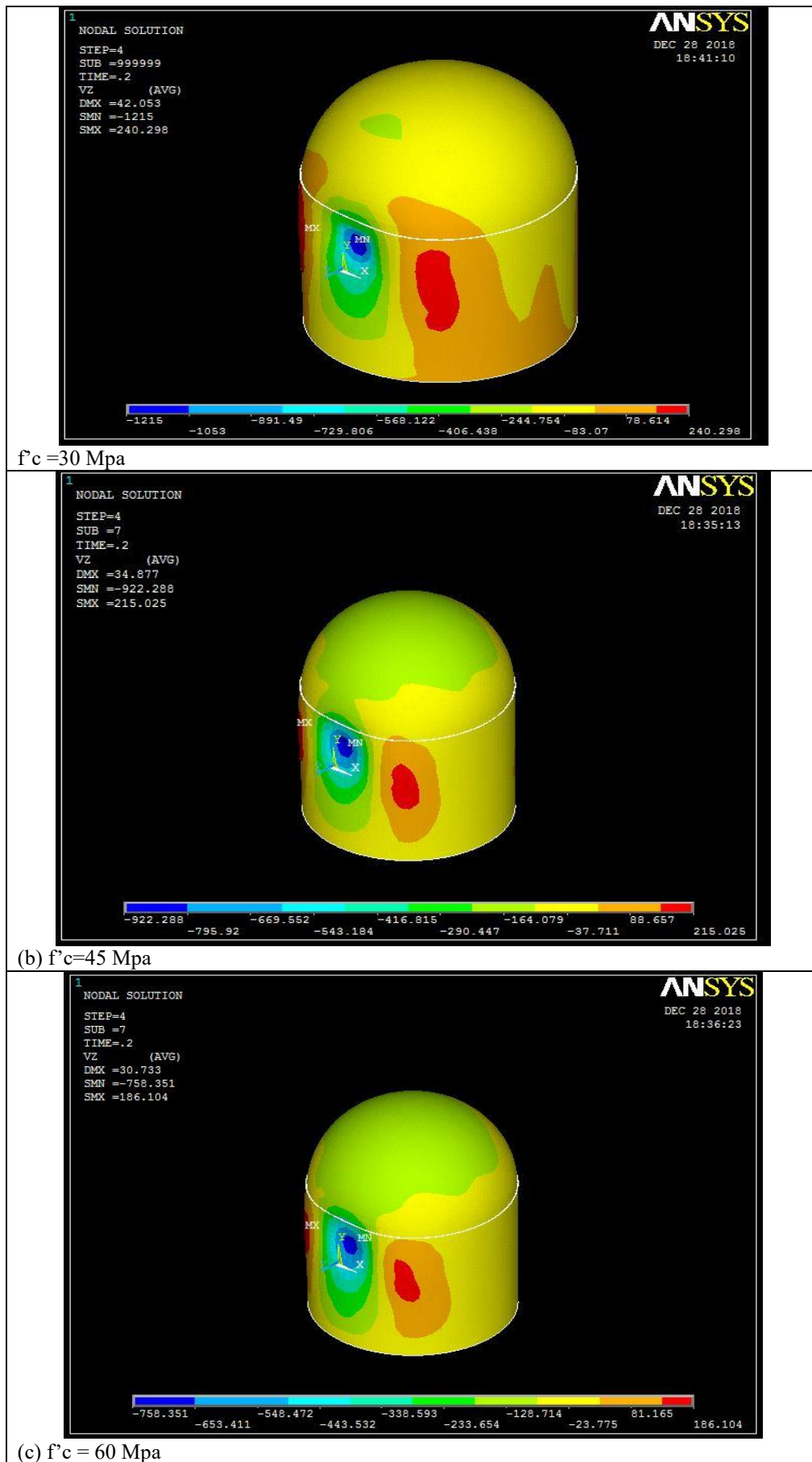
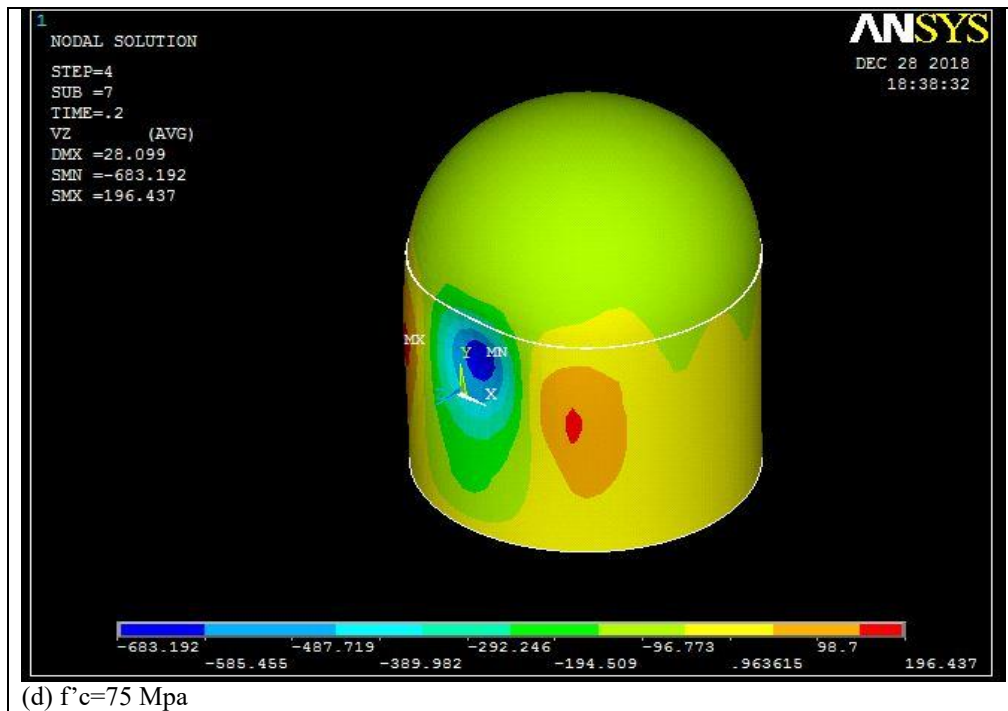


Fig 20: Displacement of RC Containment w.r.t Distance Away from Impact for Different compressive strength Due to Impact of Boeing 707-320 @ Time of Impact 0.2 Second

Velocity of RC containment due to impact of an aeroplane Boeing 707-320 moving with a speed of 103 m/sec within the impact region reached a maximum value as shown in Fig 21(a) at time 0.2 second of impact. Maximum velocity reached a value of 1215

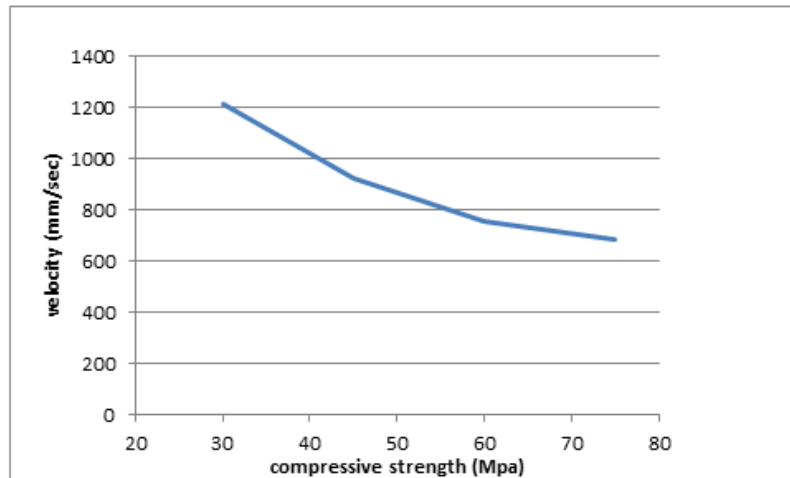
mm/sec within the impact region at time of 0.2 second with a compressive strength of 30Mpa. The velocity reached a value of 683.19 mm/sec within the impact region at time of 0.2 second for a compressive strength of 75Mpa as shown in Fig 21(d).



(d) $f'_c=75$ Mpa**Fig 21: Shapes of Velocity for RC Containments @ Different Compressive Strength @ time of impact 0.2 second**

Velocity of RC containment is 1215mm/sec when the compressive strength is 30 Mpa. Furthermore, velocity of RC containment is 683.19 mm/sec when the compressive strength is 75 Mpa. The velocity value is increased from by 77.84 % when the compressive

strength is 30 Mpa compared to compressive strength which is equal to 75 Mpa as shown in Fig 22. It is recommended to make a compressive strength for the external RC containment vessels higher than 75 Mpa.

**Fig 22: Velocity of RC Containment Versus Different Compressive Strength @ Time of Impact 0.2 second**

The maximum velocity of the RC containment due to impact of Boeing 707-320 is equal to 1207.6 mm/ sec when the compressive strength is equal to 30

Mpa within the impact region and the velocity vanished after 20m away from the impact region from each side as shown in Fig 23.

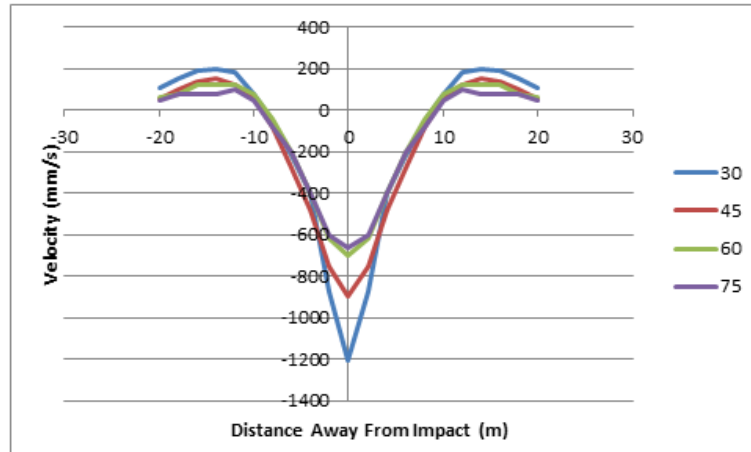
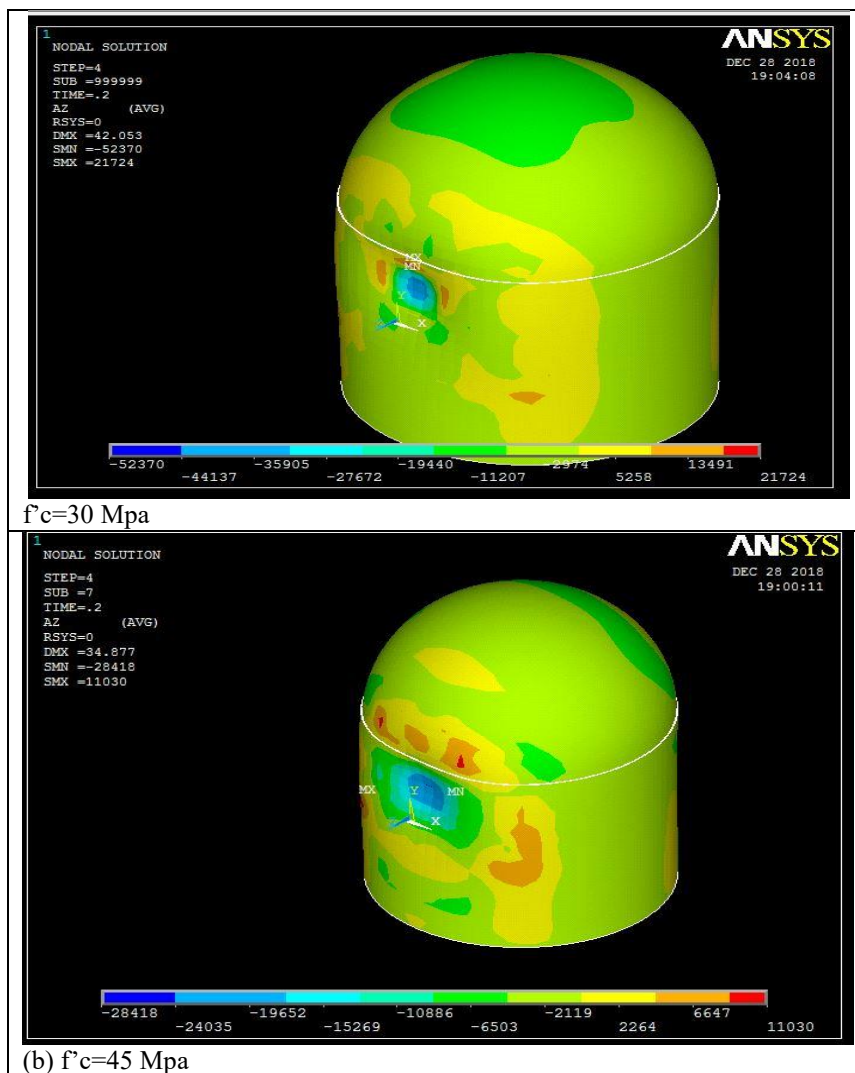


Fig 23: Velocity of RC Containment w.r.t Distance Away from Impact for Different Compressive Strength Due to Impact of Boeing 707-320 @ time of 0.2 second

Acceleration of RC containment due to impact of an aeroplane Boeing 707-320 which is moving with a speed of 103 m/sec within the impact region reached a maximum value as shown in Fig 24 at time 0.2 second of impact. Maximum acceleration reached a value of

40000 mm/sec² within the impact region at time 0.2 second with compressive strength of 30 Mpa. Acceleration reached a value of 15162 mm/sec² within the impact region at time of 0.2 second for concrete with compressive strength is equal to 75 Mpa.



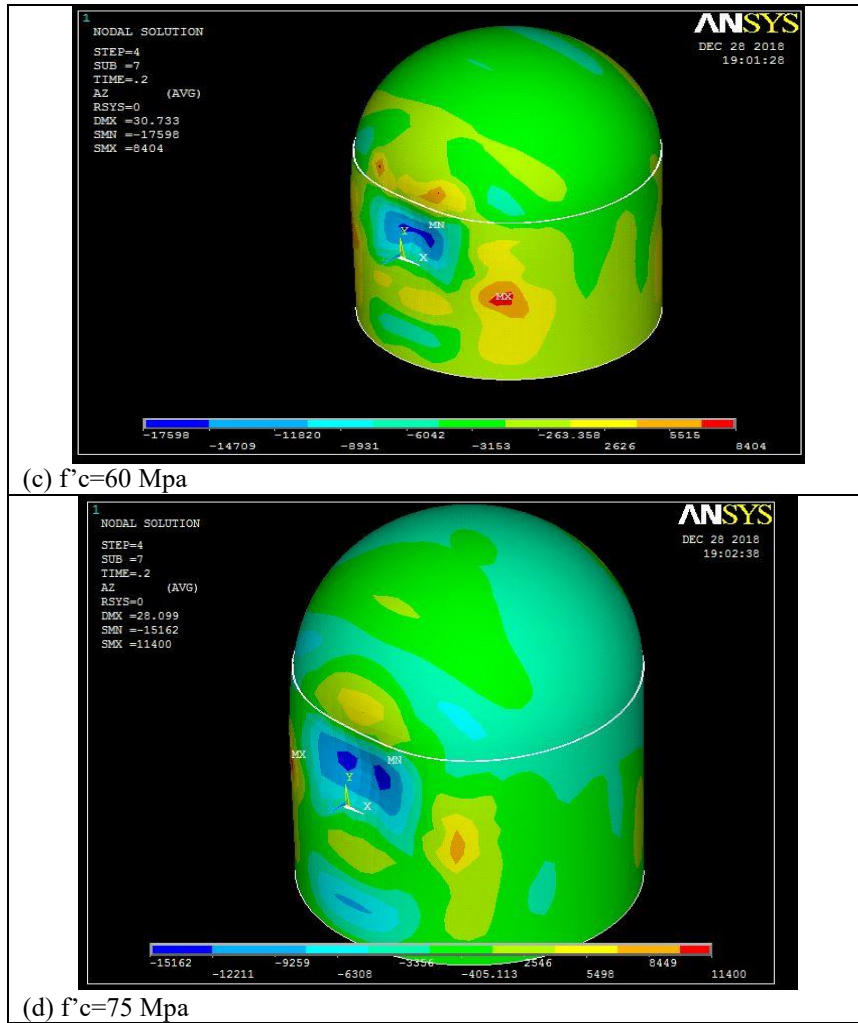


Fig 24: Acceleration Shapes of RC Containments for Different Concrete Compressive Strength

Acceleration of external RC containment is 40000 mm/sec^2 when the compressive strength is 30 Mpa. Moreover, acceleration of RC containment is 15162 mm/sec^2 when the compressive strength is 75

Mpa. The acceleration value is increased by 163.81% when the compressive strength is equal to 30 Mpa compared to concrete with compressive strength of 75 Mpa as shown in Fig 25.

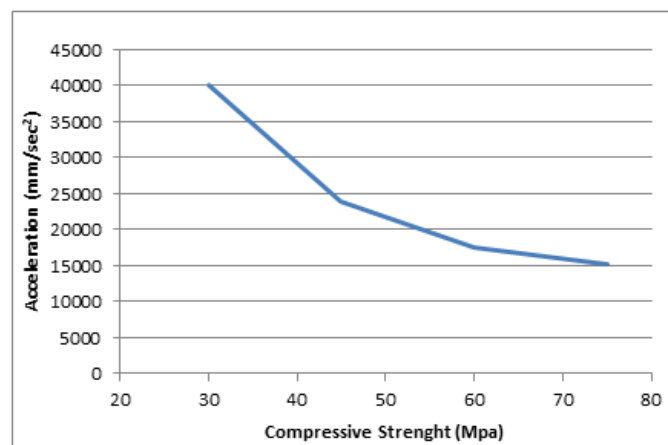


Fig 25: Acceleration of RC Containment Versus Different Compressive Strength @ Time of Impact of 0.2 second

The maximum acceleration of RC containment due to impact of Boeing 707-320 is within the impact region and the acceleration vanished after 20m away

from the impact region from each side as shown in Fig. 26 for different concrete compressive strength.

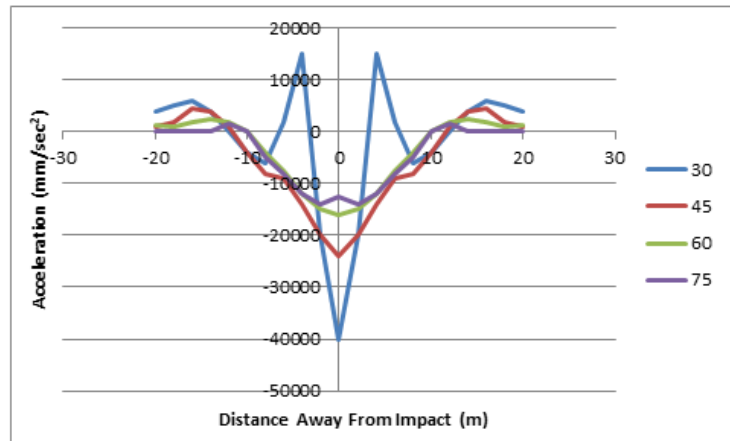
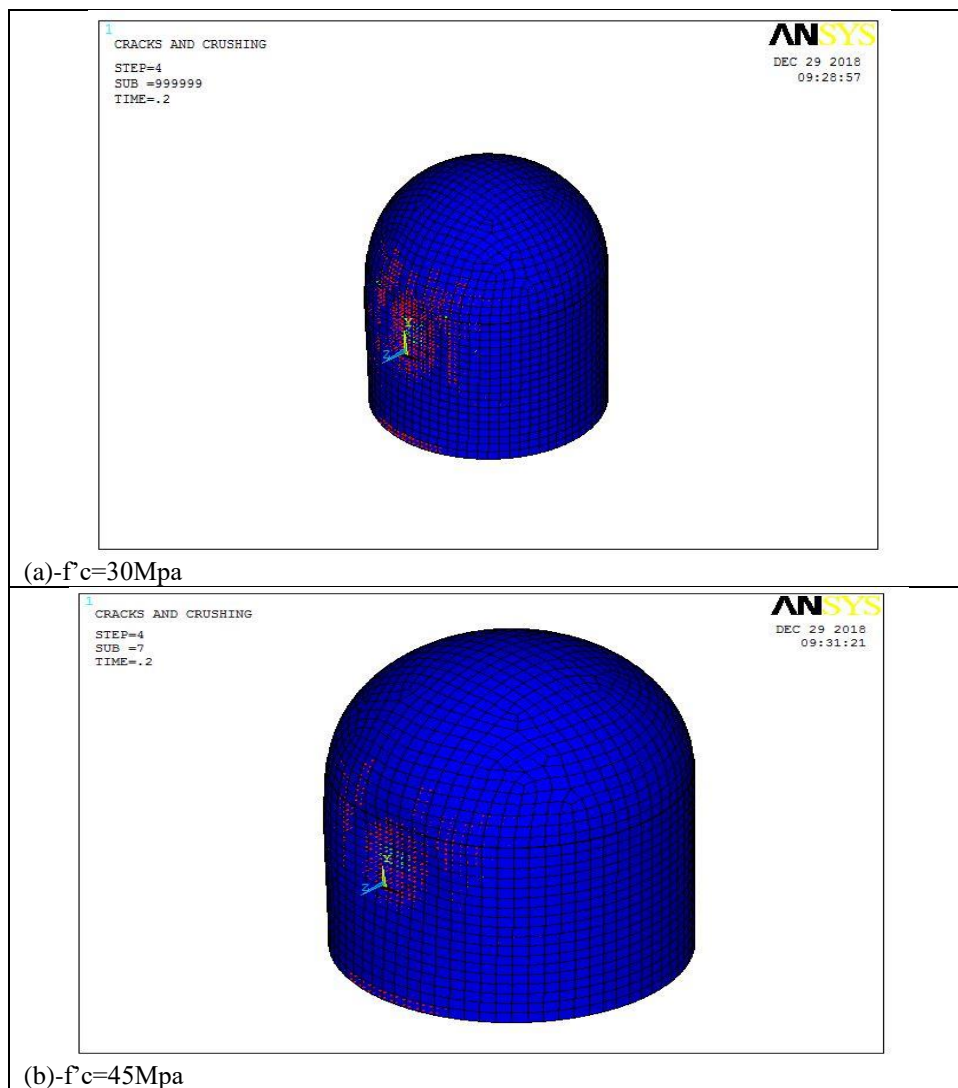


Fig 26: Acceleration of RC Containment w.r.t Distance Away from Impact with Different Compressive Strength Due to Impact of Boeing 707-320 @ time of 0.2 second

The shape of cracks for RC containment with different compressive strength due to impact of Boeing 707-320 moving with a speed of 103 m/sec are shown in Fig 27. Crushing of concrete occurred within the impact region of an aeroplane. Shear cracks appeared

away from impact region in diagonal shape. Flexure cracks appeared at the fixation of cylindrical wall with the foundation. It can be concluded from the shapes of cracks the extent of damage and cracks increases as compressive strength decreases as shown in Fig 27.



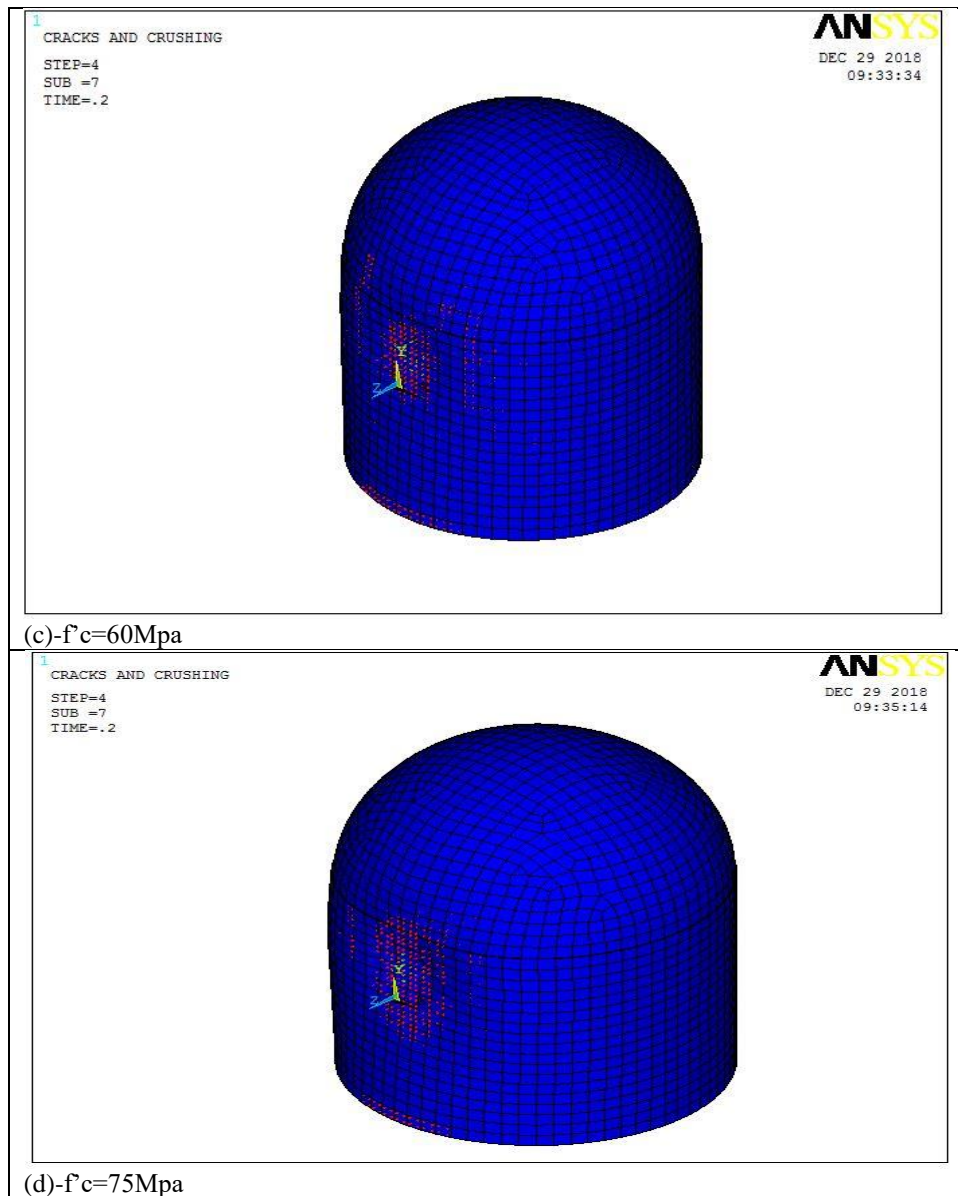


Fig 27: Shapes of Cracks for RC Containments @ Different Concrete Compressive Strength Due to Impact of Boeing 707-320

The effect of inner steel liner plate has a great effect on displacement, velocity and acceleration for RC external containment of nuclear power plant due to impact of Boeing 707-320 on exterior RC containment of NPP for a concrete with compressive strength of 60 Mpa. The parametric study is to model external RC containment of NPP using ANSYS software, one model having inner steel liner plate of thickness 0.9375cm according to ASCE 58, (1980) which is attached to the external RC containment at the inner face which is modelled using SOLID 45 element according to

ANSYS at which having a yield stress of 165 Mpa according to Teh Hu and Liang, (2015) and the other model is simulated without inner steel liner plate. In addition, it was observed that the effect of inner steel liner plate on displacement, velocity and acceleration is greater than by 22.845%, 49.421% and 100% respectively with compared to the model which doesn't contain the inner steel liner plate at time of 0.2 second of impact of an aeroplane Boeing 707-320 as shown in Figure 28.

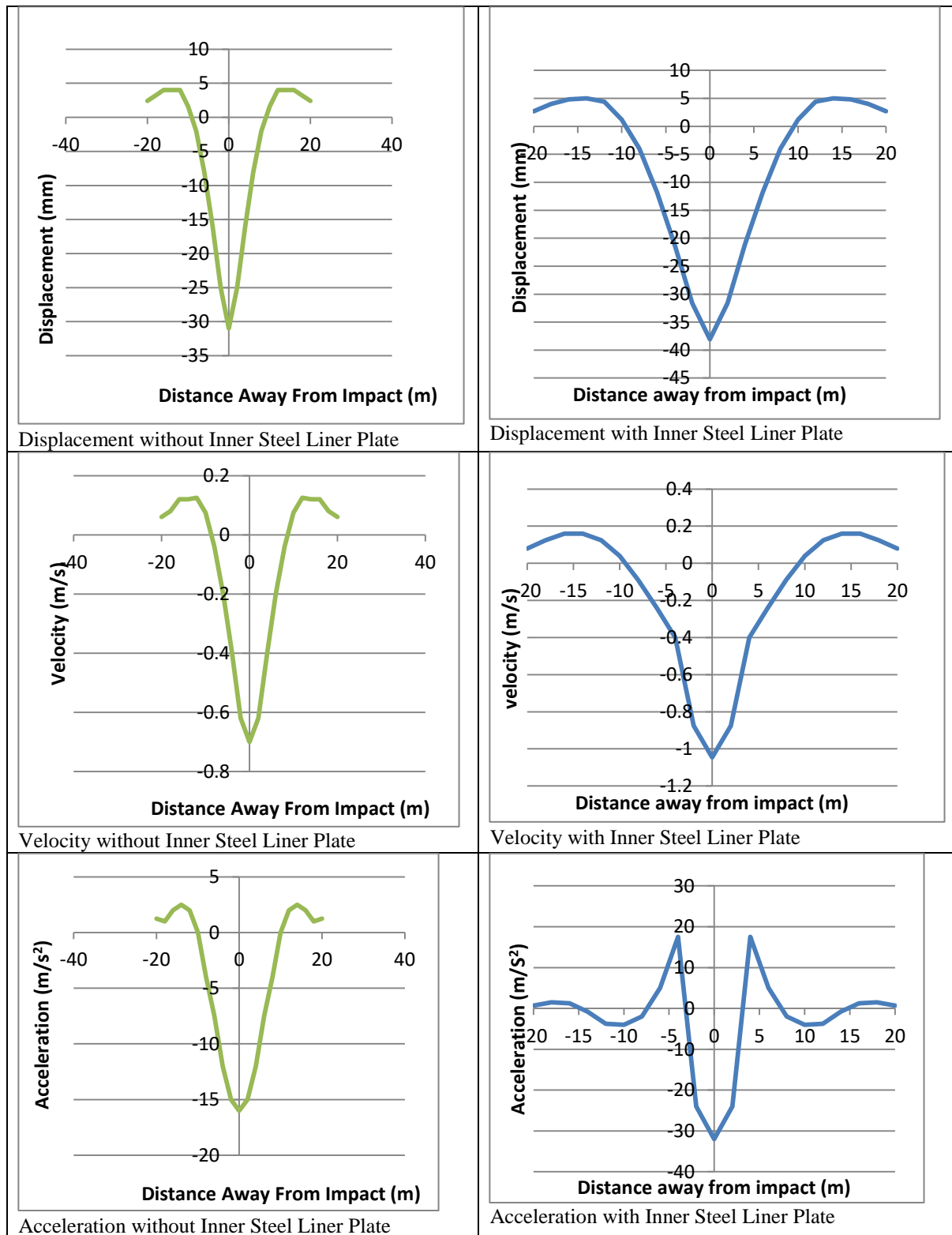


Figure 28: Comparison between the effect of steel liner for external RC containment of NPPs on Displacement, Velocity and Acceleration compared to model without Inner steel liner

4. CONCLUSION AND RECOMMENDATION

It was observed that the impact region is clearly damage from the tangential stress which appeared on the outer nodes of the impact as it mentioned before and reached a value of 30 Mpa in the tangential direction which means concrete has been

crushed at the outer nodes of concrete within the impact region. It was observed that the tangential strain reached a value of $1.7\text{E-}3$ at the inner nodes of concrete within the impact region which means concrete at the inner nodes within the impact region has been cracked. The failure criteria of concrete have been applied at the

inner nodes of concrete within the impact region and it was concluded that the concrete is cracked in two directions perpendicular to 1st and 2nd principle stresses. It was conducted that RC containment is fully intact after the impact of an aeroplane except the impact region. It was observed that the maximum displacement, velocity and the acceleration reached the maximum value within the impact region a value of 42.03 mm, 1214.06 mm/sec and 40000 mm/sec² respectively towards the direction of loading. Maximum displacement, velocity and acceleration reached a maximum value within the impact region due to impact of an aeroplane Boeing 707-320. From all the above mentioned reasons, the shear diagonal cracks appear away from the impact and the flexure cracks appear at the bottom of fixation of the cylindrical wall with the foundation. A parametric study was conducted on this paper using different compressive strength which includes (30-45-60-75) Mpa on different RC containment models hitting by an aeroplane Boeing 707-320 in order to conclude its effect on displacement, velocity and acceleration. It was concluded that the displacement, velocity and acceleration increased by 49.6%, 77.84 %, 163.81 % respectively when the compressive strength is 30 Mpa compared to compressive strength of 75 Mpa. The extent of distribution of cracks in the RC numerical model with 30Mpa compressive strength is greater than the distribution of cracks in the RC numerical model with 75Mpa according to its distribution as mentioned before. It is recommended to use the compressive higher than 75 Mpa for typical external RC containment vessel of nuclear power plants. Moreover, it was observed that the effect of inner steel liner plate on displacement, velocity and acceleration is greater than by 22.845%, 49.421% and 100% respectively with compared to the model which doesn't include the inner steel liner at time of 0.2 second of impact of an aeroplane Boeing 707-320.

REFERENCES

- ASCE standard 58, Structural Analysis and Design of Nuclear Plant Facilities 1980.
- Czerniewski, S. (2009). The Feasibility of Modern Technologies for Reinforced Concrete Containment Structures of Nuclear Power Plants, Report of Master Science 09, KANSAS State University.
- Forasassi, G., & Lofrano, R. (2010). Preliminary analysis of fan aircraft impact. A Report of Ricerca Di Sistema Elettrico.
- Němec, I., Sychrová, Š., Ševčík, I., Kabeláč, J., & Weis, L. (2012). Study of a nuclear power plant containment damage caused by impact of a plane. *International Refereed Journal of Engineering and Science (IRJES)*, 1(4), 48-53.
- Mehta, K. P., & Monteiro, P. J. (2006). Concrete Microstructure, Properties, and Materials, Electronic Book, McGraw-Hill Education, 529-531.
- Abbas, H., Paul, D. K., Godbole, P. N., & Nayak, G. C. (1996). Aircraft crash upon outer containment of nuclear power plant. *Nuclear Engineering and Design*, 160(1-2), 13-50.
- Saberi, R., Alinejad, M., Mahdavi, M. O., & Sepanloo, K. (2017). Numerical analysis of nuclear power plant structure subjected to aircraft crash. *International Journal of Advanced Structural Engineering*, 9(4), 341-352.
- Salman, W. D. (2015). Nonlinear Behaviour of Reinforced Concrete Continuous Deep Beam, *International Journal of Engineering Research & Technology (IJERT)*, 4, 2278-2281.
- ACI standard 318. Building Code Requirements for Structural Concrete 2008.
- ANSYS12.1, Theory Reference Manual 2012.
- William, K. J., & Warkne, E. P. (1974). Constitutive model for the tri-axial behaviour of concrete. In *Proceeding of the international association for bridge and structural engineering* (Vol. 19).
- Riera, J. D. (1968). On the stress analysis of structures subjected to aircraft impact forces. *Nuclear Engineering and Design*, 8(4), 415-426.
- James, R. J., & Rashid, J. Y. R. (2005, September). Severe impact dynamics of reinforced concrete structures. In *Sixth European Conference on Structural Dynamics*.
- Siefert, A., & Henkel, F. O. (2014). Nonlinear analysis of commercial aircraft impact on a reactor building—Comparison between integral and decoupled crash simulation. *Nuclear Engineering and Design*, 269, 130-135.
- Hu, H. T., & Liang, J. I. (2000). Ultimate analysis of BWR Mark III reinforced concrete containment subjected to internal pressure. *Nuclear Engineering and Design*, 195(1), 1-11.